Effects of quantum size and potential shape on the spectra of an electron and a donor in quantum dots

Jia-Lin Zhu and Jian Wu
Institute for Materials Research, Tohoku University, Sendai 980-77, Japan
and Department of Physics, Tsinghua University, Beijing 100084, China

R. T. Fu,* Hao Chen,* and Yoshiyuki Kawazoe
Institute for Materials Research, Tohoku University, Sendai 980-77, Japan
(Received 13 June 1996)

Spectra of electron and donor states in quantum dots with different confinement potentials are calculated. The potential-shape, quantum-size, and donor-position effects on the level ordering and binding are studied in detail. It is found that a single donor can heavily change single-electron spectra in the quantum dots with proper size and potential shape, which may be useful for understanding physical phenomena and designing materials and devices in quantum-dot structures. [S0163-1829(97)01704-9]

I. INTRODUCTION

Stimulated by interest in physics and technological applications of low-dimensional structures and materials, the designs, manufacture, and studies have proliferated at an explosive rate. Numerous studies have been devoted to various aspects of the electronic states associated with quasi-two-dimensional (Q2D) quantum wells, quasi-one-dimensional (Q1D) quantum-well wires, quasi-zero-dimensional (Q0D) quantum dots, and clusters.

Recently, advances in nanofabrication technology have made it possible to manufacture quantum dots (QD's) and all kinds of element clusters in which the motion of electrons is confined in all three spatial dimensions. Because of the reduced dimensionality, quantum confinement and novel transport behaviors can be observed.[1–7] In the meantime, a large number of theoretical investigations of electronic structures and related magnetic and optical properties in QD's and clusters[8–23] have been performed to explain the experimental observations.

In the Q0D structures, the single-electron spectrum plays an essential role and is gainable by studying the capacitance spectroscopy,[6,7] far-infrared spectroscopy,[1–3] conductance,[4] and other experimental results.[5] Furthermore, an atom (impurity) can change significantly the single-electron spectrum under proper Q0D structures. For example, the electronic structures of the endohedral fullerenes such as $Li@C_{60}$, $Na@C_{60}$, $La@C_{60}$, and $La@C_{82}$ (Refs. 19–23) can be quite different from those of the pure fullerenes. In general, the impurity effects on single-electron spectra are strongly related to important aspects of many-electron effects in the Q0D structures which have been studied by several authors.[14–17]

There are two interesting problems in the Q0D structures. The first is how to let an atom (impurity) enter into the Q0D structures, for example, how to form the endohedral fullerenes which have attracted considerable interest. Very recently, the first theoretical work concerning the formation process of the endohedral C_{60} has been done by using *ab initio* molecular dynamics simulation.[24] The second, as mentioned above, is how an atom (impurity) changes the single-electron spectrum in Q0D structures. In this paper, it will be presented and discussed based on calculated spectra of electron and donor states in semiconductor QD's.

The semiconductor QD's are quite idealistic Q0D structures to study, since the effective-mass theory can be used in a proper regime of quantum size. As is well known, studying the impurity states in quantum-well structures with and without strong magnetic fields is an important problem in semiconductor physics. Quantum wells, in fact, with strong magnetic fields can form some kind of QD's. Therefore the studies of donor states in $Ga_{1-x}Al_xAs$ QD's are of interest both in their own right and to understand the role of an impurity in Q0D structures.

For semiconductor QD's, two interesting idealistic models are spherical quantum dots in three-dimensional space with a rectangular potential and circular quantum disks in two-dimensional space with a parabolic potential, which have been used by a number of authors because of the high symmetry. However, a realistic quantum dot is usually deviated from spherical and circular ones while its potential, i.e., the confinement potential, is usually deviated from square and parabolic ones.[25,26] The high symmetry, in fact, can also be broken if the impurity is not located in the center of QD's. It should be interesting therefore to do a systematic investigation of the dependence of confined electron and donor states in the Q0D structures with less symmetry on the potential shape and quantum size.

The impurity states in Q2D quantum wells and Q1D quantum-well wires have been studied by a number of authors. Presently, the electronic structures in Q0D QD's, especially the donor and acceptor states, have received much attention.[8–13,18] To our knowledge, however, there has been no such systematic investigation related to the potential-shape, quantum-size, and donor-position effects on the electronic structures in QD's and the role of a single donor in the spectra under different quantum confinement conditions. It should be worthwhile to study theoretically these interesting subjects.

In Sec. II of this paper, the Hamiltonian of an electron and a donor in a quantum dot with different potential shapes is presented. In Sec. III, the exact and variational solutions are briefly shown for a donor located on the QD center and out of the center, respectively. Main results are given and discussed in Sec. IV, followed by a summary in Sec. V.

II. HAMILTONIAN

Within the framework of an effective-mass approximation, the Hamiltonian of an electron or a hydrogenic donor located in the center of a GaAs-$Ga_{1-x}Al_xAs$ spherical quantum dot can be written as

$$H_0 = -\nabla^2 - \frac{2w}{r} + V(r), \tag{1}$$

where w is equal to 0 and 1 for the electron and the donor, respectively. The potential $V(r)$ is taken to be spherically symmetric in the present work and has the form

$$V(r) = \begin{cases} V_0 & \text{if } r \geqslant R_0 \\ \alpha r^k & \text{if } r < R_0, \end{cases} \tag{2}$$

where V_0 is the barrier height and can be obtained from a fixed ratio Q of the band-gap discontinuity ΔE_g between GaAs and $Ga_{1-x}Al_xAs$, i.e., $V_0 = Q\Delta E_g$.[27] α is equal to V_0/R_0^k. The shape of $V(r)$ is determined by k as shown in Fig. 1(a).

However, the donor can be located anywhere. Let a donor be situated at $\vec{D}$ from the center of the quantum dot as shown in Fig. 1(b). In general, we can put the impurity on the Z axis, and write the Hamiltonian in the form

$$H = -\nabla^2 - \frac{2w}{|\vec{r} - \vec{D}|} + V(r). \tag{3}$$

Then the Hamiltonian can be rewritten as

$$H = H_0 + H', \tag{4}$$

with

$$H' = \frac{2w}{r} - \frac{2w}{|\vec{r} - \vec{D}|}. \tag{5}$$

In this paper, the effective atomic units are used so that all energies are measured in units of effective Rydberg R^* and all distances are measured in units of effective Bohr radius a^*. The R^* and a^* can be determined by $m^*e^4/2\hbar^2\epsilon^2$ and $\epsilon\hbar^2/m^*e^2$, where m^* and ϵ are, respectively, the electronic effective mass and the dielectric constant of GaAs materials. Here, we assume that the effective mass of $Ga_{1-x}Al_xAs$ is the same as that of GaAs. The polarization and image charge effects have been ignored because of the smaller difference of the dielectric constant between the two materials.[18]

III. EXACT AND VARIATIONAL SOLUTIONS

The eigenstates of H_0 can be labeled by the principal, orbital, and magnetic quantum numbers n, l, and m. The wave functions are written in the form

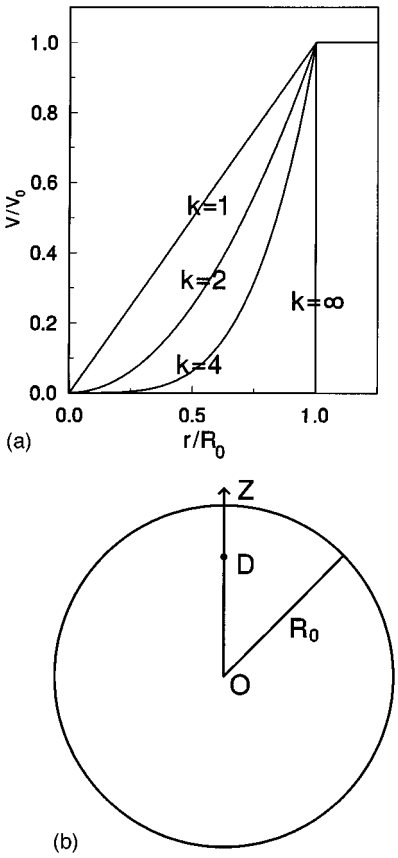

FIG. 1. (a) Profile of the potential shape of QD's of Eq. (2) for $k = 1$, 2, 4, and ∞, respectively. (b) Geometry for the problem of the donor located from the center of the dot by a distance D. The Z axis is defined by the center of the dot and the position of the donor ion.

$$\Psi_{nlm} = R_{nl}(r)Y_{lm}(\theta,\varphi), \tag{6}$$

where $Y_{lm}(\theta,\varphi)$ is the spherical harmonic function. For $V(r)$ of Eq. (2), the radial equation is found as

$$\begin{aligned} & r^2\frac{d^2R_l(r)}{dr^2} + 2r\frac{dR_l(r)}{dr} \\ & \quad + [(E_l - \alpha r^k)r^2 - l(l+1) + 2wr]R_l(r) = 0 \\ & \quad \text{for } r < R_0 \\ & r^2\frac{d^2R_l(r)}{dr^2} + 2r\frac{dR_l(r)}{dr} \\ & \quad + [(E_l - V_0)r^2 - l(l+1) + 2wr]R_l(r) = 0 \\ & \quad \text{for } r \geqslant R_0. \end{aligned} \tag{7}$$

We are prevented from obtaining analytically exact solutions of the eigenvalue problem with both Coulomb and confinement potentials. However, using the method of series expansion,[8] we can obtain exact series forms in different regions of Eq. (7). In principle, the detailed formulas, which are different from previous ones,[8] can be produced straightforwardly without any difficulty, so they are not shown here.

Using the matching conditions for different series forms in different regions, we can obtain the equation for eigenen-

TABLE I. Confined-electron spectra Q_{nl} normalized by $E_{30}(w=0)$ for QD's of $V_0=80R^*$ and $R_0=3a^*$.

	$Q_{nl}=E_{nl}(w=0)/E_{30}(w=0)$									
	$1s$	$2p$	$3d$	$2s$	$4f$	$3p$	$5g$	$4d$	$6h$	$3s$
$k=\infty$	0.111	0.228	0.374	0.445	0.550	0.672	0.754	0.931	0.986	1.000
$k=4$	0.179	0.335	0.511	0.548	0.703	0.755	0.909	0.972	1.069	1.000
	$1s$	$2p$	$2s$	$3d$	$3p$	$4f$	$3s$	$4d$	$5g$	$4p$
$k=2$	0.273	0.455	0.636	0.636	0.818	0.818	1.000	1.000	1.000	1.182
$k=1$	0.424	0.609	0.740	0.770	0.885	0.915	1.000	1.020	1.050	1.124

ergies easily and, then, the eigenenergies E_{nl} and wave functions. Compared with the cases in one, two, and three dimensions, the binding energies $E_B(n,l)$ of the donor states in the QD's are given by

$$E_B(n,l)=E_{nl}(w=0)-E_{nl}(w=1), \tag{8}$$

where $E_{nl}(w=0)$ and $E_{nl}(w=1)$ are, respectively, the corresponding eigenenergies of an electron and a donor in the QD's.

For the symmetry as shown in Fig. 1(b), the eigenstates of H can be labeled by magnetic (m) quantum numbers. Because the radius and angle variables do not separate, approximation methods should be used to obtain the eigenvalues.

Let us consider a linear variational function of the form

$$\Psi_m=\sum_{i=1}^{f} c_i\psi_i, \tag{9}$$

where ψ_i is the ith exact normorthogonal eigenstate of H_0 with eigenenergy $E_{n_il_i}(w=1)$ which is degenerate with respect to the magnetic quantum numbers. The principal, orbital, and magnetic quantum numbers of ψ_i are n_i, l_i, and m_i, respectively. In the problem considered, the summation in Eq. (9) includes only the terms with a fixed magnetic quantum number m, i.e., $m_1=m_2=\cdots=m_f=m$. In addition, it is interesting to point out that ψ_i and $\nabla\psi_i/m^*$ (Ref. 8) and, then, Ψ_m and $\nabla\Psi_m/m^*$ are, respectively, continuous at $r=R_0$.

According to the variational principle, it is straightforward to obtain the equation

$$\sum_{j=1}^{f}[H'_{ij}-(E-E_j)\delta_{ij}]c_j=0, \quad i=1,2,\ldots,f \tag{10}$$

with

$$H'_{ij}=\langle\psi_i|H'|\psi_j\rangle. \tag{11}$$

Substituting Eq. (6) into Eq. (11), we can find H'_{ij} in the form

$$H'_{ij}=2w\int_0^\infty R_{n_il_i}(r)R_{n_jl_j}(r)r\,dr\,\delta_{l_il_j}-2\sum_{l=|l_i-l_j|}^{l_i+l_j}(-1)^m[(2l_i+1)(2l_j+1)]^{1/2}\begin{bmatrix} l_i & l_j & l\\ 0 & 0 & 0\end{bmatrix}\begin{bmatrix} l_i & l_j & l\\ -m & m & l\end{bmatrix}$$
$$\times\left(\frac{1}{D^{l+1}}\int_0^D R_{n_il_i}(r)R_{n_jl_j}(r)r^{l+2}dr+D^l\int_0^D R_{n_il_i}(r)R_{n_jl_j}(r)\frac{1}{r^{l-1}}dr\right), \tag{12}$$

where

$$\begin{bmatrix} l_i & l_j & l\\ -m & m & l\end{bmatrix}$$

is the Wigner 3-j symbol.

The condition that this set of Eqs. (10) has nonzero solution leads to the secular equation of finite degree f,

$$||H'-B||=0, \tag{13}$$

where matrix elements of H' are H'_{ij} of Eq. (12) and B is a diagonal matrix, i.e.,

$$B_{ij}=(E-E_j)\delta_{ij}, \quad i,j=1,2,\ldots,f. \tag{14}$$

Then, the energy levels are obtained by solving Eq. (13) numerically. For $\vec{D}\neq\vec{0}$, they can be denoted by E_{nlm} even though l is not a good quantum number. E_{nlm} is degenerate with respect to m and $-m$, and E_{nl0} is nondegenerate. The binding energy $E_B(n,l,m)$ can be defined by

$$E_B(n,l,m)=E_{nl}(w=0)-E_{nlm}. \tag{15}$$

IV. RESULTS AND DISCUSSION

In order to show the potential-shape (k), quantum-size (R_0), and donor-position (D) effects on single-electron spectra in QD's and to better understand the important role of a single impurity in the spectra, we have calculated energy levels of electron and donor states in QD's of $V_0=80R^*$ as a function of k, R_0, and D, respectively.

TABLE II. Confined-donor spectra W_{nl} normalized by $E_{30}(w=0)$ for QD's of $V_0=80R^*$ and $R_0=3a^*$.

	$W_{nl}=E_{nl}(w=1)/E_{30}(w=0)$									
	$1s$	$2p$	$2s$	$3d$	$4f$	$3p$	$5g$	$3s$	$4d$	$6h$
$k=\infty$	−0.095	0.093	0.217	0.258	0.443	0.504	0.653	0.748	0.787	0.888
$k=4$	0.031	0.237	0.408	0.429	0.631	0.655	0.843	0.866	0.889	1.012
	$1s$	$2p$	$2s$	$3d$	$3p$	$4f$	$3s$	$4d$	$5g$	$4p$
$k=2$	0.143	0.373	0.534	0.572	0.746	0.763	0.910	0.941	0.951	1.115
$k=1$	0.314	0.545	0.667	0.722	0.834	0.876	0.941	0.976	1.016	1.081

A. k, R_0, and D effects on spectra

In Tables I and II, we have shown the spectra of QD's with $R_0=3a^*$ and $V_0=80R^*$. The k is equal to 1, 2, 4, and ∞, respectively. Here Q_{nl} and W_{nl} stand for the energy levels of electron and donor states with the well-defined quantum number n and l, normalized with the corresponding value of $3s$ electron level $E_{30}(w=0)$ in the QD's. The value of $E_{30}(w=0)$ is equal to 49.2753, 32.7957, 21.1506, and 9.1599 R^* for $k=1$, 2, 4, and ∞, respectively. It is clearly seen that the energy-level structure is dramatically changed as the k changes from 1 to ∞. An important aspect of the potential-shape effects is the changes of the level ordering, which would have an influence on the magic number of superatoms. As illustrated in Table I, the ordering of electron states in the QD of $k=\infty$, i.e., a square well, is $1s$, $2p$, $3d$, $2s$, $4f$, $3p$, $5g$, $4d$, $6h$, $3s$, and so on, while that of $k=1$ is $1s$, $2p$, $2s$, $3d$, $3p$, $4f$, $3s$, and so on. It shows that the lower levels of the superatoms are dominated by no-radial-node states of $1s$, $2p$, $3d$, and so on, and that there are much more no-radial-node states in the lower levels for the QD's with larger k than for those with smaller k. Such a potential-shape effect can be useful in electronic device applications.

For an isolated donor, i.e., without the confinement potential, the ordering of the energy levels is $1s$, $2s$ $(2p)$, $3s$ $(3p, 3d)$, $4s$ $(4p, 4d, 4f)$, ... As the confinement potential exists, the levels with the same principal number n split. The stronger the confinement potential is, the larger the level splitting is. It could be expected that the ordering of donor levels in QD's will be quite different from that of isolated donor levels for a strong confinement and all the same as that of the corresponding electron levels for a very strong confinement. It is more complex for an intermediate confinement. As shown in Tables I and II, the ordering of electron levels Q_{nl} and donor levels W_{nl} can be quite different from that of isolated donor levels. The orderings of W_{nl} of $k=4$ and ∞ are not the same as that of the corresponding Q_{nl} and the difference between the W_{nl} and Q_{nl} is larger for $k=\infty$ than for $k=4$. However, the orderings of W_{nl} and Q_{nl} are the same for $k=1$ and 2, respectively.

As shown in Table I, the orderings of Q_{nl} are the same for $k=1$ and 2 and are about the same for $k=4$ and ∞. Only the difference between them exists in $6h$ and $3s$ levels. In Table II, the orderings of W_{nl} are the same for $k=4$ and ∞, so are those for $k=1$ and 2, and there are some changes in the ordering as the k changes from 2 to 4. It is obvious that the $4f$ level is higher and lower than the $3p$ level for $k=2$ and 4, respectively. The same phenomenon occurs in the group of $3s$, $4d$, and $5g$ levels. Besides the level sequence, the transition energy between two levels is different for different k. It means that the potential shapes have a great influence on the electronic structure of QD's.

Comparing Table II with Table I, it is easy to find the existence of a donor in QD's can change the energy levels effectively. For example, two segments of the sequence are $3d$, $2s$ and $4d$, $3s$ for $k=\infty$ in Table I, and $2s$, $3d$ and $3s$, $4d$ for $k=\infty$ in Table II. In these cases, the introduction of a single donor changes the ordering of s and d states. In addition, the effectiveness of the impurity to change the sequence is different for different k. For instance, the alteration for $k=1$ and 2 is smaller than that for $k=4$ and ∞.

Using $R_0=1a^*$ instead of $R_0=3a^*$ in the calculations above, we have obtained the ordering of W_{nl} which is all the same to that of the corresponding Q_{nl}. It means that the quantum size has obvious effects on the ordering, and that the role of a single impurity is dependent on the R_0 and k in determining the energy levels.

In Figs. 2(a) and 2(b), we have plotted the spectrum of a donor in QD's of $V_0=80R^*$ with $k=\infty$ and the levels of $2s$ and $3d$ states of a donor in QD's of $V_0=80R^*$ with $k=1,2,4,\infty$ as a function of R_0, respectively. Here, for the sake of clearness, the spectrum and the levels are also normalized with the corresponding value of $3s$ electron level $E_{30}(w=0)$ in the QD's with the R_0. In Fig. 2(a), it is readily seen that the crossover of $2s$, $3d$, and $3s$ with $4d$ states occurs as R_0 changes from $0.5a^*$ to $3.5a^*$. An intersection of $2s$ and $3d$ states occurs for $k=4$ and the level separation at $R_0=1$ and $3a^*$ is smaller for $k=4$ than for $k=\infty$ as shown in Fig. 2(b). It is also shown that there is no intersection of $2s$ and $3d$ states for $k=1$ and 2. However, there is an intersection of $3s$ and $4f$ states for all of $k=1$, 2, 4, and ∞ at some points not shown here. What has been mentioned above shows the strong R_0 and k coupling effects on the donor spectra. The reason can be understood if the characteristics of electron levels and wave functions and, then, binding energies determined by different confinement potentials of QD's are noted. It will be discussed in the next part of this section.

In order to understand the role of a single impurity in single-electron spectra of QD's much better, in Fig. 3, we have plotted the ground and excited energy levels of a donor as a function of D for QD's of $R_0=3a^*$ and $V_0=80R^*$ with $k=\infty$, and only the states with $m=0,\pm1,\pm2$ are shown. The splitting of energy levels can be easily seen from the figure as the impurity ion is removed from the center. For example, p states are split into two levels with $m=0$ and ±1 and d states into three levels with $m=0$, ±1, and ±2. It is inter-

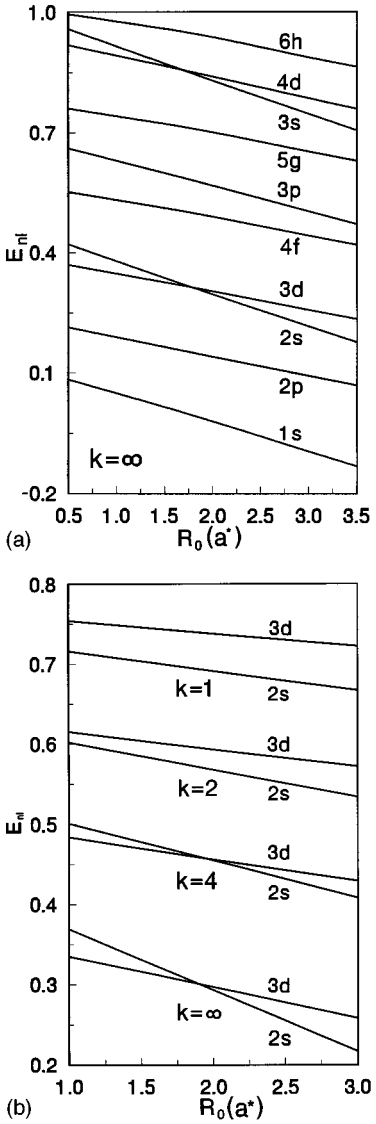

FIG. 2. (a) Energy levels $E_{nl}(w=1)$ of center donor in QD's of $V_0=80R^*$ with $k=\infty$ as a function of R_0. (b) $2s$ and $3d$ levels in QD's of $V_0=80R^*$ with $k=1$, 2, 4, and ∞ as a function of R_0, respectively.

esting to note that E_{nl0} is the lowest level among E_{nlm}. However, there is no splitting for s states. All of the energy levels approach the exact ones $E_{nl}(w=1)$ as D approaches zero. On the other hand, the $l+1$ splitting levels come near and approach $E_{nl}(w=0)$ as D approaches infinity. The above picture is the same for the case of QD's with $k=2$.

An obvious feature of Fig. 3 is the intersection of $2s$ state with $3d$ state and those of $3s$ state with $4d$ and $6h$ states, which alter the sequence. The crossover of $2s$ and $3d$ occurs at about $0.7a^*$, and those of $3s$, $4d$ and $3s$, $6h$ are at about $0.4a^*$ and $1.2a^*$, respectively. It is a result of the coupling and competition of Coulomb potential with the confinement one. Moreover, the effect of two potentials on energy levels is related to the corresponding wave functions. Only s state wave functions have nonzero values at the origin, so the Coulomb potential around the center has greater influence on s states than others. This is the reason the energies of s states change more remarkably along with changing D than the

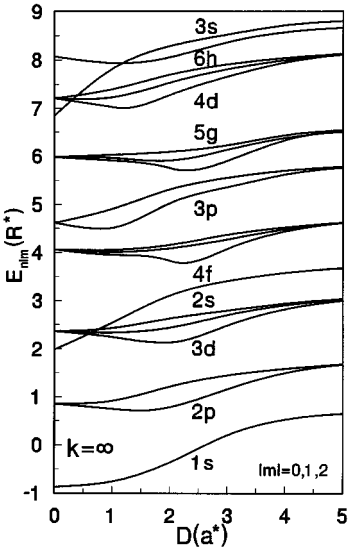

FIG. 3. Energy levels E_{nlm} of an off-center donor in a quantum dot of $V_0=80R^*$ and $R_0=3a^*$ with $k=\infty$ as a function of D. Here $|m|$ is taken to be equal to 0, 1, and 2 only.

others. In the same region of R_0, however, there are no such intersections for QD's with $k=2$. It can be easily understood if we note that there is no difference of the level ordering between Q_{nl} and W_{nl} of QD's with $k=2$ in Tables I and II.

Using $R_0=1a^*$ instead of $R_0=3a^*$ in the calculations above, we have found that there is the splitting of energy levels too as the impurity ion is removed from the center. However, there is no intersection for $2s$, $3d$ states and $3s$, $4d$ states. From $1s$ up to $3s$ and $6h$, only one intersection exists. The crossover of $3s$ and $6h$ occurs at about $0.6a^*$. Again, it means that the quantum size has obvious effects on the energy-level ordering and that the role of a single impurity is dependent on the R_0 and D in determining the ordering in QD's.

To close this part of the section, it is helpful to compare the present result of $D\neq 0$ with others. However, only the other result[12] can be found for the ground state of $D\neq 0$ in QD's with $V_0=\infty$. The ground energies for $D=0.5$ and $1a^*$ in a QD of $R_0=3a^*$ with $V_0=80R^*$ obtained in the present work are, respectively, equal to $-0.811R^*$ and $-0.748R^*$. The present result is agreeable with those ($-0.82784R^*$ and $-0.75680R^*$) in Ref. 12 since the finite-barrier effect is small for the ground states in this case.

B. Binding energies

For a better understanding of the R_0, k, and D effects, it is interesting to study the binding energies defined by Eqs. (8) and (15). In Table III, the binding energies have been shown for center ($D=0$) donor states in QD's of $V_0=80R^*$ and $R_0=3a^*$ with $k=1$, 2, 4, and ∞, respectively. We should note that the sequence of binding energies is different among different k. For example, $E_B(1,0)>E_B(2,0)>E_B(3,0)$, $E_B(2,1)>E_B(3,1)$, and $E_B(3,2)>E_B(4,2)$ for $k=1$ and 2, while $E_B(3,0)>E_B(2,0)>E_B(1,0)$, $E_B(3,1)>E_B(2,1)$, and $E_B(4,2)>E_B(3,2)$ for $k=\infty$. The characteristics of binding energies can be explained by studying the wave functions of confined electron states determined by H_0 of Eq. (1) with

TABLE III. Binding energies $E_B(n,l)$ measured in units of R^* for QD's of $V_0=80R^*$ and $R_0=3a^*$.

$k=\infty$	n,l	$3s$	$2s$	$1s$	$3p$	$4d$	$2p$	$3d$	$4f$	$5g$
	$E_B(n,l)$	2.311	2.085	1.891	1.541	1.322	1.237	1.066	0.982	0.930
$k=4$	n,l	$1s$	$2s$	$3s$	$3p$	$2p$	$4d$	$3d$	$4f$	$5g$
	$E_B(n,l)$	3.134	2.965	2.836	2.111	2.073	1.760	1.715	1.518	1.388
$k=2$	n,l	$1s$	$2s$	$3s$	$2p$	$3p$	$3d$	$4d$	$4f$	$5g$
	$E_B(n,l)$	4.248	3.369	2.956	2.673	2.380	2.110	1.951	1.798	1.594
$k=1$	n,l	$1s$	$2s$	$2p$	$3s$	$3p$	$3d$	$4d$	$4f$	$5g$
	$E_B(n,l)$	5.393	3.602	3.153	2.885	2.502	2.356	2.000	1.926	1.651

$w=0$. If a wave function shows that the electron distribution is mainly near to the center of the dot, the binding energy is large. This point of view can be formulated as follows. It is accurate enough to calculate the binding energies with the use of the first-order perturbation as the confinement potential is strong enough compared with the Coulomb potential. Then, the binding energy $E_B(n,l)$ is given by

$$E_B(n,l)=\left\langle \Psi_{nl}\left|\frac{2}{r}\right|\Psi_{nl}\right\rangle=\left\langle R_{nl}\left|\frac{2}{r}\right|R_{nl}\right\rangle, \tag{16}$$

where Ψ_{nl} and R_{nl} are, respectively, the total and radial normalized wave functions of H_0 with $w=0$. Therefore the spatial distribution of an electron on this state determines the magnitude of $E_B(n,l)$. The characteristics of binding energies mentioned above are unchanged as the confinement is strong and, then, the first-order perturbation is valid.

As a specific example, we study the case for $k=\infty$. The radial wave function R_{nl} of $k=\infty$ with $V_0\rightarrow\infty$ is

$$R_{nl}(r)\rightarrow A_{nl}j_l[\sqrt{E_{nl}(w=0)}r], \tag{17}$$

with

$$E_{nl}(w=0)=(X_{nl}/R_0)^2, \tag{18}$$

where A_{nl} is a normalization constant, and $j_l(x)$ and X_{nl} are the lth-order spherical Bessel function and its $(n-l)$th root, respectively. It can be seen from the graph of $R_{nl}(r)$ with a fixed l that the electron is nearer to the center of the dot for larger n (the node number is $n_r=n-l-1$) than for smaller ones, that is to say, the electron is attracted by the donor ion more strongly for large n and, then, $E_B(n+2,l)>E_B(n+1,l)>E_B(n,l)$ and so on.

Another example is for $k=2$ with $V_0\rightarrow\infty$. The radial wave function is

$$R_{nl}(r)\rightarrow B_{nl}r^l e^{-\sqrt{\alpha}r^2}F(-n(n-l-1),l+3/2,2\sqrt{\alpha}r^2), \tag{19}$$

where $F(a,b,z)$ is the confluent hypergeometric function and B_{nl} is a normalization constant. The graph of R_{nl} with a fixed l shows that the electron is nearer to the center of the dot for smaller n than for larger ones. So the binding energies increase with decreasing n for the same l, i.e., $E_B(n,l)>E_B(n+1,l)>E_B(n+2,l)$ and so on.

Based on what has been mentioned above, we can better understand the dependence of the sequence of the binding energies on k shown in Table III and, then, the ordering difference between Q_{nl} and W_{nl} of $k=\infty$ and 2 shown in Tables I and II.

For the strong confinement, the electron levels and the binding energies are almost in proportion to $1/R_0^2$ and $1/R_0$, respectively. Therefore, changing R_0 from a smaller value to a larger one, we can have an intersection for two levels if one of them with a larger binding energy is higher than the other with a smaller binding energy in the strong confinement condition. Otherwise, there is no intersection for the two levels. According to Tables I, II, and III, we can now understand what has been mentioned for $2s$, $3d$ states [Fig. 2(b)] and $3s$ and $4f$ states in Sec. IV A much better.

For $\vec{D}\neq\vec{0}$ case, it is found that the binding energy $E_B(n,l,m)$ defined in Eq. (15) reduces with increasing $|m|$ for fixed n and l and it is consistent with the ordering shown in Fig. 3. Furthermore, the binding energies with $|m|=l$ reduce monotonously with increasing $\vec{D}$, while the others have maximum binding energies at some D not equal to zero. The maximum value is larger for smaller $|m|$. The above characteristic feature can be explained as follows. According to the angular distribution of wave functions, the states with $m=0$ mainly distribute along the z axis and the other states are more and more distant from the z axis with increasing $|m|$. So, the donor ion influences the state with smaller $|m|$ more effectively and, then, a larger binding energy is gained. This is the reason we have the picture of the spectrum as shown in Fig. 3.

V. SUMMARY

Using the methods of series expansion and linear variational calculations, we have reported the calculated results of spectra of electron and donor confined by GaAs-$Ga_{1-x}Al_xAs$ QD's. The results have clearly demonstrated the k, R_0, and D effects. These effects can be understood better on the basis of analyzing the characteristics of wave functions and, then, binding energies in different QD's.

The competing and coupling between confinement and impurity potential are different for different R_0. When the R_0 of a QD is large, the donor spectra are similar to those of an isolated donor. When the R_0 becomes much smaller, the spectra are similar to those of an electron in the QD. For the intermediary radius, the impurity and confinement potential are coupled strongly. In this region the crossover for some levels happens. When the R_0 is changed from a large to a small value, some of the lower energy levels can intersect with higher ones and it changes the level ordering. This reflects that R_0 is an important factor to determine the electronic structures.

The effects of a single impurity on the level ordering and

binding energies are strongly dependent not only on the R_0 but also on the k. The k is also an important factor in investigating the properties of QD's, such as magic number, magnetism, and optical transitions, which may be clarified.

For an off-center donor ($D \neq 0$), the splitting and ordering of quantum levels are dependent on k, R_0, and D. The most interesting and inspiring feature of D dependence of the energy-level structure is the intersection of some levels. It means that a single impurity can largely change the single-electron spectrum of a QD and, then, the property.

To close this paper, it is interesting to point out that the k, R_0, and D effects are not only important for single-electron spectra but also for two- and many-electron spectra in QD's since the two- and many-electron spectra are strongly related to the single-electron spectra. For example, a proper design of the potential shape and the radius of a QD may enhance the electron spin polarization very effectively utilizing the spin-orbit interaction.[28] The ground states of a negative donor center in asymmetric quantum wells with strong magnetic fields[29] are quite different from that of a negative donor center in symmetric quantum wells with the same fields. Therefore, in order to understand the physical phenomena in Q0D structures better and to use the quantum-size, potential-shape, and impurity effects in designing materials and devices of QD's, it should be worthwhile to study these effects on two- and many-electron spectra of QD's. Work on the effects on two-electron spectra is in progress.

ACKNOWLEDGMENTS

The authors would like to thank the Information Science Group of the Institute for Materials Research, Tohoku University for their continuous support of the supercomputing system. One of the authors (J.L.Z.) would like to thank the Materials Design Virtual Laboratory (IBM Hitachi) for financial support.

*Permanent address: Department of Physics, Fudan University, Shanghai 200433, China.

[1] C. Sikorski and U. Merkt, Phys. Rev. Lett. **62**, 2164 (1989).
[2] T. Demel, D. Heitmann, P. Grambow, and K. Ploog, Phys. Rev. Lett. **64**, 788 (1990).
[3] A. Lorke, J.P. Kotthaus, and K. Ploog, Phys. Rev. Lett. **64**, 2559 (1990).
[4] P.L. McEuen, E.B. Foxman, U. Meirav, M.A. Kastner, Y. Meir, N.S. Wingreen, and S.J. Wind, Phys. Rev. Lett. **66**, 1926 (1991).
[5] M.A. Kastner, Rev. Mod. Phys. **64**, 849 (1992).
[6] R.C. Ashoori, H.L. Stormer, J.S. Weiner, L.N. Pfeiffer, S.J. Pearton, K.W. Baldwin, and K.W. West, Phys. Rev. Lett. **68**, 3088 (1992).
[7] R.C. Ashoori, H.L. Stormer, J.S. Weiner, L.N. Pfeiffer, K.W. Baldwin, and K.W. West, Phys. Rev. Lett. **71**, 613 (1993).
[8] J.L. Zhu, Phys. Rev. B **39**, 8780 (1989); J.L. Zhu, J.J. Xiong, and B.L. Gu, *ibid.* **41**, 6001 (1990).
[9] G.T. Einevoll and Y.C. Chang, Phys. Rev. B **40**, 9683 (1989).
[10] G.T. Einevoll, Phys. Rev. B **45**, 3410 (1992).
[11] D.S. Chuu, C.M. Hsiao, and W.N. Mei, Phys. Rev. B **46**, 3898 (1992).
[12] K.R. Brownstein, Phys. Rev. Lett. **71**, 1427 (1993).
[13] Y. Kayanuma and H. Momiji, Phys. Rev. B **41**, 10 261 (1990).
[14] P.A. Maksym and T. Chakraborty, Phys. Rev. Lett. **65**, 108 (1990).
[15] N.F. Johnson and M.C. Payne, Phys. Rev. Lett. **67**, 1157 (1991).
[16] M. Wagner, U. Merkt, and A.V. Chaplik, Phys. Rev. B **45**, 1951 (1992).
[17] S.R.E. Yang, A.H. MacDonald, and M.D. Johnson, Phys. Rev. Lett. **71**, 3194 (1993).
[18] C.R. Proetto, Phys. Rev. Lett. **76**, 2824 (1996).
[19] P.P. Schmidt *et al.*, J. Phys. Chem. **95**, 10537 (1991).
[20] J. Cioslowski and E.D. Fleischmann, J. Chem. Phys. **94**, 3730 (1991).
[21] A. Rosén and B. Wästberg, J. Am. Chem. Soc. **110**, 8701 (1988).
[22] A.H.H. Chang *et al.*, J. Chem. Phys. **94**, 5004 (1991).
[23] S. Nagase and K. Kaboyashi, Chem. Phys. Lett. **214**, 57 (1993).
[24] K. Ohno, Y. Maruyama, K. Esfarjani, Y. Kawazoe, N. Sato, R. Hatakeyama, T. Hirata, and M. Niwano, Phys. Rev. Lett. **76**, 3590 (1996).
[25] M. Tewordt, V.J. Law, M.J. Kelly, R. Newbury, M. Pepper, D.C. Peacock, J.E.F. Frost, D.A. Ritchie, and G.A.C. Jones, J. Phys. Condens. Matter **2**, 8969 (1990).
[26] B. Meurer, D. Heitmann, and K. Ploog, Phys. Rev. Lett. **68**, 1371 (1992).
[27] S. Adachi, J. Appl. Phys. **58**, R1 (1985).
[28] S. Nagano, Phys. Rev. B **50**, 7962 (1994).
[29] J.L. Zhu, D.L. Lin, and Y. Kawazoe, Phys. Rev. B (to be published).